

Unified 2D and 3D Pre-Training of Molecular Representations

Jinhua Zhu*
teslazhu@mail.ustc.edu.cn
University of Science and Technology
of China
Hefei, Anhui, China

Yingce Xia†
yingce.xia@microsoft.com
Microsoft Research Asia
Beijing, China

Lijun Wu
lijuwu@microsoft.com
Microsoft Research Asia
Beijing, China

Shufang Xie
shufxi@microsoft.com
Microsoft Research Asia
Beijing, China

Tao Qin
taoqin@microsoft.com
Microsoft Research Asia
Beijing, China

Wengang Zhou
zhwg@ustc.edu.cn
University of Science and Technology
of China
Hefei, Anhui, China

Houqiang Li
lihq@ustc.edu.cn
University of Science and Technology
of China
Hefei, Anhui, China

Tie-Yan Liu
tyliu@microsoft.com
Microsoft Research Asia
Beijing, China

ABSTRACT

Molecular representation learning has attracted much attention recently. A molecule can be viewed as a 2D graph with nodes/atoms connected by edges/bonds, and can also be represented by a 3D conformation with 3-dimensional coordinates of all atoms. We note that most previous work handles 2D and 3D information separately, while jointly leveraging these two sources may foster a more informative representation. In this work, we explore this appealing idea and propose a new representation learning method based on a unified 2D and 3D pre-training. Atom coordinates and interatomic distances are encoded and then fused with atomic representations through graph neural networks. The model is pre-trained on three tasks: reconstruction of masked atoms and coordinates, 3D conformation generation conditioned on 2D graph, and 2D graph generation conditioned on 3D conformation. We evaluate our method on 11 downstream molecular property prediction tasks: 7 with 2D information only and 4 with both 2D and 3D information. Our method achieves state-of-the-art results on 10 tasks, and the average improvement on 2D-only tasks is 8.3%. Our method also achieves significant improvement on two 3D conformation generation tasks.

CCS CONCEPTS

• **Applied computing** → *Molecular structural biology; Bioinformatics*; • **Computing methodologies** → **Machine learning**.

*This work was done when Jinhua Zhu was an intern at Microsoft Research Asia.
†Corresponding author.

Permission to make digital or hard copies of all or part of this work for personal or classroom use is granted without fee provided that copies are not made or distributed for profit or commercial advantage and that copies bear this notice and the full citation on the first page. Copyrights for components of this work owned by others than the author(s) must be honored. Abstracting with credit is permitted. To copy otherwise, or republish, to post on servers or to redistribute to lists, requires prior specific permission and/or a fee. Request permissions from [permissions@acm.org](https://www.acm.org).
KDD '22, August 14–18, 2022, Washington, DC, USA
© 2022 Copyright held by the owner/author(s). Publication rights licensed to ACM.
ACM ISBN 978-1-4503-9385-0/22/08...\$15.00
<https://doi.org/10.1145/3534678.3539368>

KEYWORDS

Molecule pre-training; molecular property prediction; conformation generation

ACM Reference Format:

Jinhua Zhu, Yingce Xia, Lijun Wu, Shufang Xie, Tao Qin, Wengang Zhou, Houqiang Li, and Tie-Yan Liu. 2022. Unified 2D and 3D Pre-Training of Molecular Representations. In *Proceedings of the 28th ACM SIGKDD Conference on Knowledge Discovery and Data Mining (KDD '22)*, August 14–18, 2022, Washington, DC, USA. ACM, New York, NY, USA, 11 pages. <https://doi.org/10.1145/3534678.3539368>

1 INTRODUCTION

Deep learning techniques have attracted more and more attention recently in drug discovery [17, 38], bioinformatics [32] and cheminformatics [39]. Obtaining effective molecular representations, usually high dimensional vectors that are friendly to neural network models, is a key prerequisite for deep learning based methods [6, 23].

Molecules can be expressed in different forms, including 2D molecular graphs and 3D molecular conformations. A 2D molecular graph describes the 2D topological structure of a molecule, where the nodes/atoms are connected by edges/bonds respectively. Many methods have been proposed to deal with molecular graphs such as Graphormer [48], virtual node [11], etc. A 3D molecular conformation is represented by a set of coordinates for all the atoms of a molecule. People also propose various models based on 3D conformations, such as SchNet [31], DimeNet [20], PAiNN [30], etc.

While the two types of representations are complementary, i.e., 2D graphs focus on topological connections of atoms and 3D conformations focus on spatial arrangements of atoms, only limited works leverage them together. Chen et al. [4] use the multiscale weighted colored algebraic graphs (AG) to encode 3D conformation and obtain corresponding 3D representations. Besides, they use a bidirectional Transformer [6, 40] to encode the molecular SMILES [43]

(obtained by traversing a 2D molecular graph using depth-first-search) and obtain another representation. The two representations are fused together for downstream tasks. Liu et al. [22] and Stärk et al. [36] are two recent works that use both 2D information and 3D information for molecule pre-training. Their common training objective is to maximize the mutual information between the 2D and 3D views of a molecule, where the 2D view and 3D view are encoded using two different modules.

Different from above methods [4, 22, 37], in this work, we propose a unified method that processes both 2D and 3D information of molecules in a single model, inspired by the recent trend and success of multi-modality modeling in deep learning research [18, 28]. For examples, DALL-E [28] is a unified model that can encode images and texts together, and demonstrates its great power in text-to-image generation; Kaiser et al. [18] use one unified model for image, speech and text processing, and show that the tasks with less data benefit largely from the joint training.

Our model is pre-trained on PCQM4Mv2 [13], where molecules are represented by both 2D graphs and corresponding 3D conformations. In our model, atomic coordinates and interatomic distances are encoded by a feed-forward network and then fused by a graph neural network. To effectively unify 2D and 3D information, we design several pre-training tasks:

(1) Reconstruction of masked atoms and coordinates, which is to reconstruct randomly masked atoms and coordinates based on unmasked ones;

(2) 3D conformation generation conditioned on 2D graph, which is to generate 3D conformation based on the 2D graph of a molecule;

(3) 2D graph generation conditioned on 3D conformation, which is to generate 2D graph based on the 3D conformation of a molecule.

We use masked language modeling loss [6, 23] to reconstruct the masked atoms. Besides, we adopt a permutation invariant loss function of symmetric substructures so that the training process is more effective. This is because the coordinates of atoms in symmetric substructures can be swapped, and conventional loss function cannot maintain permutation invariance. We also adopt the roto-translation invariance loss to 3D conformation generation conditioned on the 2D graph. Note that our model is compatible with molecules with 2D information only, where their coordinates can be randomly initialized.

We test our method on the following tasks:

(1) Six molecular property prediction tasks from MoleculeNet [45] and one molecular prediction tasks from OGB benchmark¹ [14]. The 3D conformations of these molecules are not accessible.

(2) Four toxicity prediction tasks from [4, 44] where both 2D and 3D information are available.

(3) Two 3D molecular conformation tasks where the data is sampled from the Geometric Ensemble Of Molecules dataset [3, 33].

We achieve state-of-the-art results on 10 out of the 11 molecular property prediction tasks. Specifically, on the 2D-only tasks, we improve the previous best method by 8.3% on average. For the toxicity prediction with 3D conformations, our method outperforms the previous deep learning based methods and the manually designed 3D molecular fingerprints. For the two conformation generation tasks

on GEOM-QM9 and GEOM-Drugs, in terms of the mean matching score, we improve the previous best results by 7.7% and 3.6%.

Our contributions can be summarized as follows:

(1) We propose a new method that jointly encodes both 2D and 3D information of molecules in a unified model. The learnt model can be used for both molecular prediction and conformation generation tasks.

(2) We propose several new training objective functions to fully utilize the data, which shows new directions of molecule pre-training.

(3) We achieve state-of-the-art results on 10 molecular prediction tasks and 2 conformation generation tasks.

(4) We release our code and pre-trained models at the Github repository <https://github.com/teslacool/UnifiedMolPretrain> for reproducibility.

2 RELATED WORK

2.1 Molecular Pre-training with 2D Information

Inspired by its success in natural language processing and computer vision, pre-training has been introduced into molecular representation learning recently. In these works, a molecule is represented by either a SMILES [43] sequence or an undirected graph where the nodes and edges are atoms and bonds, respectively. By using SMILES sequence, Chithrananda et al. [5], Wang et al. [41] use the masked language modeling objective [6] for pre-training. Honda et al. [12] learn molecular representation by reconstructing the input SMILES with a Transformer based on a sequence-to-sequence model. By regarding a molecule as a graph, Hu et al. [15] perform node-level and graph-level pre-training, which are about to reconstruct the masked attributes and preserve the consistency of similar subgraphs. Wang et al. [42] use contrastive learning, where the representation of a molecule m should be similar to the augmented version of m while dissimilar to others. GraphCL [49] uses graph augmentation and contrastive learning for pre-training. Rong et al. [29] design GNN Transformer for pre-training, which extends the attention blocks to graph data. They also use two new training objective functions, one is to predict the motifs in a graph, and the other is to predict the subgraph property represented by a well-designed string. Zhu et al. [52] propose to maximize the consistency between SMILES representation and graph representation, and achieve remarkable performance on several downstream tasks.

2.2 3D Molecular Representation

Encoding 3D spatial structure into molecular representation is important to determine molecular property. Anderson et al. [2], Lu et al. [24], Schütt et al. [31] take the atomic distance into consideration and design a set of novel architecture to deal with atomic positions. Klicpera et al. [20], Shui and Karypis [34] further involve bond angle into their methods and achieve better performance. Recently, Fuchs et al. [9], Schütt et al. [30] introduce equivariant networks to ensure the equivariance of molecular representation under continuous 3D roto-translations.

¹https://ogb.stanford.edu/docs/leader_graphprop/

2.3 Molecular Pre-training with 3D Information

Recently, there emerge several works for molecule pre-training with 3D spatial structure. Chen et al. [4] use the element-specific multi-scale weighted colored algebraic graph (AG) to embed the chemical and physical interactions into graph invariants and capture 3D molecular structural information, which is then fused with the complementary bi-directional Transformer representation. Stärk et al. [36] propose to implicitly encode the 3D information into molecular representation by maximizing the mutual information between a 2D graph representation and a 3D representation which are produced by two separate networks. Liu et al. [22] propose the Graph Multi-View Pre-training (GraphMVP) framework, which leverages contrastive learning and molecule reconstruction (under the variational auto-encoder framework) for pre-training. To our best knowledge, almost all previous works encode 2D graph and 3D structure with different backbone models, and we are the first to encode them using a unified model.

3 OUR METHOD

3.1 Notations

Let $G = (V, E)$ denote a 2D molecular graph, where $V = \{v_1, v_2, \dots, v_{|V|}\}$ is a collection of atoms, and E is a collection of bonds. Let e_{ij} denote the bond between atom v_i and v_j . Let $R \in \mathbb{R}^{|V| \times 3}$ denote the 3D conformation of molecule G , where the i -th row R is the coordinate of atom v_i . For ease of reference, when the context is clear, we use V to denote the indices of atoms, i.e., $V = \{1, 2, \dots, |V|\}$.

Let $\text{FF}(\dots)$ denote a two-layer feed-forward network with ReLU activation and Batch Normalization [16]. The input of $\text{FF}(\dots)$ is the concatenation of all input tensors, and the output is a d -dimensional vector, where d is the dimension of the network hidden states.

3.2 Training Objective

The overall training objective functions consist of three parts: reconstruction of masked atoms and coordinates; 3D conformation generation conditioned on 2D graph and 2D graph generation conditioned on 3D conformation. The illustration is in Figure 1.

3.2.1 Reconstruction of masked atoms and coordinates.

Given a molecule G with $|V|$ nodes and the corresponding conformation R , with probability $p \in (0, 1)$, each atom v_i is independently masked. Also, the coordinate of each atom v_j , i.e., R_j , is independently masked. Denote the indices of the unmasked atoms and coordinates as I_a and I_c , respectively. The task is to reconstruct the masked tokens (i.e., $V \setminus I_a$ and $V \setminus I_c$) based on unmasked ones (i.e., I_a and I_c). The training objective for reconstructing the masked atoms is:

$$\ell_{\text{atom}} = \sum_{i \in V \setminus I_a} \log P(v_i | \{v_j\}_{j \in I_a}; \{R_j\}_{j \in I_c}), \quad (1)$$

which is similar to that in natural language processing [6, 23] and computer vision [7].

Assume the coordinate of atom v_j is masked and let \hat{R}_j denote the predicted coordinate of atom v_j . To measure the difference between the groundtruth coordinate R_j and generated coordinate

$\hat{R}_j \forall j \in V \setminus I_c$, the most straightforward way is to use

$$\tilde{\ell} = \sum_{j \in V \setminus I_c} \|R_j - \hat{R}_j\|^2. \quad (2)$$

However, for 3D conformation, this is not the best choice because there might be symmetric molecules, where the coordinates of atoms can be swapped. An example is shown in Figure 2(a), where the molecule is symmetric along the bond between atom 4 and 5. If we swap the coordinates of atom 3, 2, 1, 0 with 6, 7, 8, 9, the conformation remains the same, but the loss in Eqn.(2) changes. In addition, although some molecules are not symmetric, they still have symmetric substructures. As shown in Figure 2(b), atoms 12, 13 are symmetric to 16, 15 along the C-C bond (atom 10 and 11). Another symmetric substructure is the piperidine at the right side of Figure 2(b). If we swap the coordinates of the symmetric substructures, the 3D conformation should remain unchanged. Such permutation invariance cannot be maintained by Eqn.(2).

When we randomly mask the coordinates, it is possible to mask the symmetric substructures. To tackle this challenge, we follow [27, 51] and use the permutation invariant loss. Given a molecule G , let α denote a bijective mapping from $\{1, 2, \dots, |V|\}$ to itself. Let \mathcal{P} denote the collection of atom mappings on symmetric substructures. For the picture in Figure 2(b), \mathcal{P} has four mappings.

- (1) $\alpha(i) = i \forall i \in V$;
- (2) $\alpha(12) = 16, \alpha(16) = 12, \alpha(13) = 15, \alpha(15) = 13$ and $\alpha(i) = i$ for remaining atoms;
- (3) $\alpha(1) = 17, \alpha(17) = 1, \alpha(0) = 18, \alpha(18) = 0$ and $\alpha(i) = i$ for remaining atoms;
- (4) $\alpha(12) = 16, \alpha(16) = 12, \alpha(13) = 15, \alpha(15) = 13, \alpha(1) = 17, \alpha(17) = 1, \alpha(0) = 18, \alpha(18) = 0, \alpha(i) = i$ for remaining atoms.

The loss function that is permutation invariant to symmetric substructures is defined as follows:

$$\ell_{\text{coord}} = \min_{\alpha \in \mathcal{P}} \sum_{j \in V \setminus I_c} \|R_j - \alpha(\hat{R}_j)\|^2, \quad (3)$$

where $R_j \in \mathbb{R}^3$ and $\alpha(\hat{R}_j) \in \mathbb{R}^3$ denote the coordinate of the j -th atom in R and $\alpha(\hat{R}_j)$, respectively. Zhu et al. [51] provide an efficient implementation to find the \mathcal{P} based on graph automorphism and we follow their method.

3.2.2 3D conformation generation conditioned on 2D graph.

We mask all the coordinates of a conformation and reconstruct them based on the 2D molecular graph only. Molecular conformation generation is an important topic for both bioinformatics and machine learning, and various methods have been proposed, including the distance-based methods [33, 35, 47] (which generate the interatomic distances or their gradients first and then reconstruct the conformation) or the direct approach (which directly outputs the 3D conformation). Recently, Zhu et al. [51] proposed a method named directly molecular conformation generation (DMCG) that outputs the coordinates directly and achieved state-of-the-art results. We use DMCG for conformation generation in our unified pre-training framework.

The conformation should maintain roto-translation invariance [26] and permutation invariance [27]. Roto-translation invariance means that if we rotate and translate the generated 3D conformation

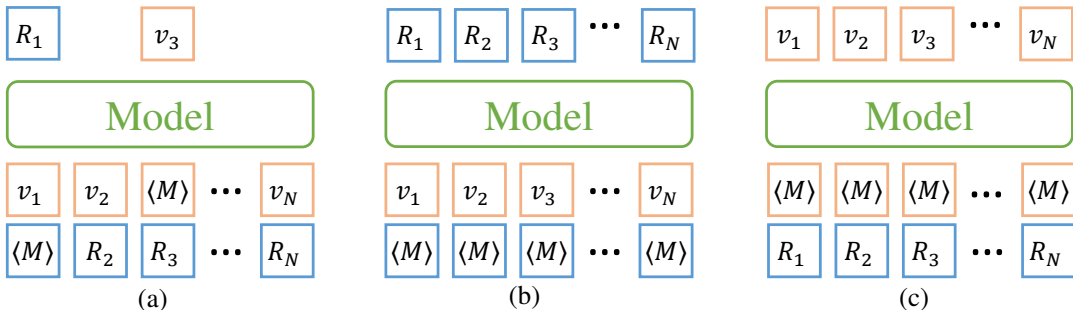


Figure 1: The training objective functions. (a) reconstruction of masked atoms and coordinates; (b) 3D conformation generation conditioned on 2D graph; (c) 2D graph generation conditioned on 3D conformation. $\langle M \rangle$ denotes the masked atoms and coordinates.

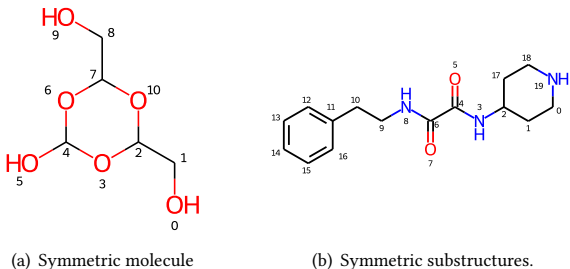


Figure 2: An example of the symmetry in molecules.

\hat{R} rigidly, the distance between \hat{R} and the groundtruth conformation R remains unchanged. The permutation invariance has been introduced in Section 3.2.1. Mathematically, the loss function is defined as follows:

$$\ell_{2D \rightarrow 3D} = \frac{1}{|V|} \min_{\varrho, \alpha \in \mathcal{P}} \sum_{i \in V} \|R_i - \varrho(\alpha(\hat{R}_i))\|^2. \quad (4)$$

In Eqn.(4), \hat{R}_i is obtained based on the 2D graph G without touching the 3D information; ϱ is the roto-translational operation. ϱ can be written as $\varrho(R) = RQ + t$, where Q is a 3×3 rotation matrix, and $t \in \mathbb{R}^{1 \times 3}$ is the transition vector. Eqn.(4) is roto-translation invariant and permutation invariant to the symmetric substructures. According to [19], calculating the minimum value over roto-translation operations can be transformed into calculating the minimum eigenvalues of some 4×4 matrix, and we use their method. More details are available in our implementation.

3.2.3 2D graph generation conditioned on 3D conformation.

We mask all atoms and reconstruct them based on the 3D conformation. The 2D structure of the molecule is kept, i.e., we know which two atoms are connected, but we do not know the bond type between them. The training objective function is defined as follows:

$$\ell_{3D \rightarrow 2D} = \frac{1}{|V|} \sum_{i \in V} \log P(v_i | \{R_j\}_{j \in V}). \quad (5)$$

Note that in Eqn.(1), only partial atoms are masked. We can reconstruct them based on the remaining atoms and coordinates. In comparison, Eqn.(5) is an extreme case where all atoms are masked,

and we need to reconstruct them purely by coordinates. Both of the two loss functions are helpful for pre-training.

3.2.4 Discussion.

Compared with the pre-training in natural language processing, ℓ_{atom} and $\ell_{3D \rightarrow 2D}$ are similar to the masked language modeling [6, 23]. However, for ℓ_{coord} and $\ell_{2D \rightarrow 3D}$, we use the permutation invariant and roto-translation invariant version. In Eqn.(3), since only partial coordinates are masked, we just need to consider the permutation invariance of symmetric atoms and do not need the roto-translational operation on all coordinates. This is because the unmasked coordinates can help reduce the roto-translation freedom. In comparison, in Eqn.(4), considering all the atoms are masked, we should consider both permutation and roto-translation invariance since we have no unmasked coordinates to align.

3.3 Network Architecture

As mentioned in Section 1, we propose a method that can encode the 2D and 3D information using one model and output a unified representation. We use the GN block module proposed by [1, 51] as our backbone due to their superior performance on molecule classification and molecular conformation generation. Denote the model as $\text{net}(G, R)$, where the inputs include the 2D graph G and 3D conformation R . The input atoms, bonds are first mapped into d -dimensional representation using the corresponding embedding layers. All the masked atoms are represented by a special embedding E_a and all the related bond embeddings are represented by another special embedding E_b , both of which are learned during pre-training. If the coordinates $R_i \in \mathbb{R}^3$ of atom i is masked, each element in R_i is replaced with a number uniformly sampled from $[-1, 1]$.

Compared with previous molecule pre-training with 2D information only, how to encode the 3D information is an important problem. Inspired by pointed Transformer [50] and the equivalent network [9], we encode both the coordinates and interatomic distances. Let x_i and \bar{x}_i denote the representations of atom i before and after combining with 3D information. Let x_{ij} and \bar{x}_{ij} denote the representations of bond e_{ij} before and after combining with 3D information. We have that

$$\bar{x}_i = x_i + \text{FF}(R_i), \quad \bar{x}_{ij} = x_{ij} + \text{FF}(\|R_i - R_j\|). \quad (6)$$

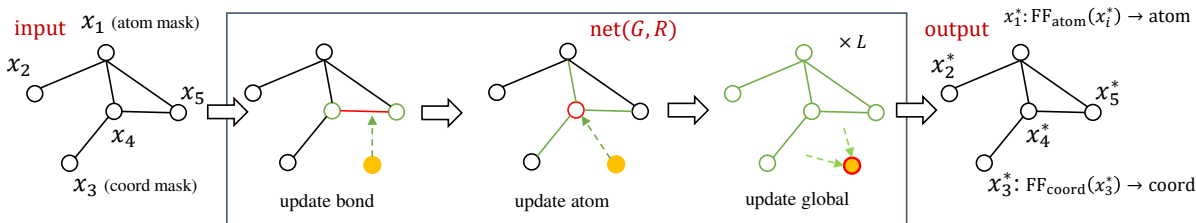


Figure 3: A brief workflow of the network architecture. For the input molecule, we mask the atom information of atom 1 and mask the coordinates of atom 3. It is then processed by a stack of L blocks, where the yellow node refers to the global representation of the molecule. We eventually obtain a representation x_i^* for each atom, based on which we can reconstruct the masked atoms and coordinates.

Note that some x_i could be the E_a , some x_{ij} could be E_b , and some coordinates R_i 's are not the real coordinates but randomly sampled. The \tilde{x}_i 's and \tilde{x}_{ij} 's are then fed into the main backbone for further processing. Briefly, $\text{net}(\dots)$ stacks L identical blocks. As shown in Figure 3, in each block, we first update the bond representations (the red edge) using the related atom representations (the green nodes) and a global representation of the molecule (the yellow node). After that, the atom representations (the red node) are updated in an attentive way using the related edge representations (the green edges) and the global representation (the yellow node). Finally, we update the global representation by averaging the updated atom and bond representations. The network $\text{net}(G, R)$ eventually outputs a representation for each atom, i.e.,

$$(x_1^*, x_2^*, \dots, x_{|V|}^*) = \text{net}(G, R). \quad (7)$$

The mathematical formulation of $\text{net}(G, R)$ is summarized in Appendix A. We use two different MLP layers to reconstruct the atoms and coordinates. Both of them take x_i^* as input:

(1) FF_{atom} , which outputs the masked atoms. It will be used in Eqn.(1) and Eqn.(5).

(2) FF_{coord} , which outputs the masked coordinates. It will be used in Eqn.(3) and Eqn.(4).

For the example in Figure 3, we mask the atom information of node x_1 and mask the coordinates of node x_3 . After obtaining their representations x_1^* and x_3^* , they are reconstructed by $\text{FF}_{\text{atom}}(x_1^*)$ and $\text{FF}_{\text{coord}}(x_3^*)$

We summarize the pre-training procedure in Algorithm 1.

Please note that [51] is for 2D molecular graph to 3D conformation generation, and their loss function is specially designed for conformation generation. In this work, our focus is to jointly use 2D/3D information and obtain effective molecular representations. Our method can be used for molecule modeling and generation.

4 APPLICATION TO PROPERTY PREDICTION

We work on 11 tasks to verify the effectiveness of our method: (1) 7 molecular property prediction tasks with 2D information only; (2) 4 molecular property prediction tasks with both 2D and 3D information.

4.1 Settings

Dataset. We use the PCQM4Mv2 dataset [13] for pre-training, which has 3.38M data. In PCQM4Mv2, both the 2D information and

Algorithm 1 Workflow of the pre-training.

- 1: *Input:* Training data (G, R) ; optimizer opt ; mask probability p ;
 - ▷ Calculate ℓ_{atom} and ℓ_{coord}
- 2: With probability p , we independently mask the atoms in G and obtain G' . The unmasked atom indices are I_a .
- 3: With probability p , we independently replace the coordinates in R with some coordinates uniformly sampled from $[-1, 1]$ to obtain R' . The indices of the original coordinates are I_c .
- 4: $(\hat{x}_1^*, \hat{x}_2^*, \dots, \hat{x}_{|V|}^*) = \text{net}(G', R')$;
- 5: If atom v_i is masked, i.e., $i \in V \setminus I_a$, $\hat{v}_i = \text{FF}_{\text{atom}}(\hat{x}_i^*)$;
- 6: If coordinate R_j is replaced, i.e., $j \in V \setminus I_c$, $\hat{R}'_j = \text{FF}_{\text{coord}}(\hat{x}_j^*)$;
- 7: Calculate the ℓ_{atom} in Eqn.(1) and the ℓ_{coord} in Eqn.(3).
 - ▷ Calculate $\ell_{2D \rightarrow 3D}$
- 8: Replace all coordinates in R with a random matrix $R'' \in \mathbb{R}^{|V| \times 3}$, where each element is uniformly sampled from $[-1, 1]$;
- 9: $(\tilde{x}_1^*, \tilde{x}_2^*, \dots, \tilde{x}_{|V|}^*) = \text{net}(G, R'')$.
- 10: $\forall i \in V, \tilde{R}_i = \text{FF}_{\text{coord}}(\tilde{x}_i^*)$.
- 11: Calculate the loss $\ell_{2D \rightarrow 3D}$ in Eqn.(4) using $\{\tilde{R}_i\}_{i \in V}$.
 - ▷ Calculate $\ell_{3D \rightarrow 2D}$
- 12: Mask all atoms and bonds in G and obtain G'' . The connection of atoms (i.e., which two atoms are connected) is kept.
- 13: $(\tilde{x}_1^*, \tilde{x}_2^*, \dots, \tilde{x}_{|V|}^*) = \text{net}(G'', R)$.
- 14: $\forall i \in V, \tilde{v}_i = \text{FF}_{\text{atom}}(\tilde{x}_i^*)$.
- 15: Calculate the loss $\ell_{3D \rightarrow 2D}$ in Eqn.(5) using $\{\tilde{v}_i\}_{i \in V}$.
 - ▷ Update the model parameter θ .
- 16: Denote the parameter of net as θ . Update the model by $\theta \leftarrow \text{opt}(\theta, \nabla_{\theta}(\ell_{\text{atom}} + \ell_{\text{coord}} + \ell_{2D \rightarrow 3D} + \ell_{3D \rightarrow 2D}))$.

3D information are available. In this dataset, each 2D molecular graph corresponds to one 3D conformation calculate by density function theory. We randomly split the dataset into training and validation sets by 95%:5%.

For molecular property prediction with 2D information only, following [22, 36], we choose six tasks on MoleculeNet [45]: BBBP, Tox21, ClinTox, HIV, BACE and SIDER. Most of them are with limited data. Following [22, 36], for each task, we split the dataset into training, validation and test sets by 8:1:1 according to their molecular scaffolds. We also conduct experiments on ogb-molpcba [14], which is a larger dataset with 438K data. All these tasks are classification tasks.

Table 1: Results on MoleculeNet, where only 2D information is available.

Dataset	BBBP	Tox21	ClinTox	HIV	BACE	SIDER	Avg
AttrMask & ContextPred [15]	71.2 ± 0.9	74.2 ± 0.8	73.7 ± 4.0	75.8 ± 1.1	78.6 ± 1.4	60.4 ± 0.6	72.31
GROVER [29]	70.3 ± 1.6	75.2 ± 0.3	77.8 ± 2.0	75.9 ± 0.9	79.2 ± 0.3	60.6 ± 1.1	73.17
GraphCL [49]	67.5 ± 3.3	75.0 ± 0.3	78.9 ± 4.2	75.0 ± 0.4	68.7 ± 7.8	60.1 ± 1.3	70.87
Stärk et al. [36]	71.1 ± 2.0	78.9 ± 0.6	59.4 ± 3.2	76.1 ± 1.1	79.4 ± 2.0	57.3 ± 5.0	70.37
GraphMVP [22]	72.4 ± 1.6	75.9 ± 0.5	77.5 ± 4.2	77.0 ± 1.2	81.2 ± 0.9	63.9 ± 1.2	74.65
Ours	77.4 ± 0.6	75.9 ± 0.3	95.4 ± 1.1	82.2 ± 1.0	86.8 ± 0.6	67.4 ± 0.5	80.85

Table 2: Results on ogb-molpcba dataset.

Method	Valid AP	Test AP
GN block [1]	0.2745	0.2650
GIN + virtual node [21]	0.2798	0.2703
Graphormer [48]	0.3227	0.3140
Ours	0.3225	0.3125
Ours + FLAG	0.3304	0.3174

For property prediction with both 2D and 3D information, following Chen et al. [4], we work on four toxicity prediction tasks: LD50, IGC50, LC50 and LC50DM, all of which are regression tasks. They measure the toxicity from different aspects. More details of the above datasets are summarized in Table 7 of the Appendix.

Training configuration. The pre-trained model has 12 layers, and the hidden dimension of each block is 256. The masked ratio p is 0.25. The model is pre-trained for 100 epochs using Adam optimizer with initial learning rate 2×10^{-4} , batch size 128 and is trained on four P40 GPUs.

For the molecular property prediction tasks with 2D information only, all the coordinates are randomly sampled from uniform distribution $[-1, 1]$. For the tasks on MoleculeNet, we use grid search to determine the learning rate, dropout and batch size, which are summarized in Appendix B. For ogb-molpcba, the learning rate is fixed as 10^{-4} and we train the model for 100 epochs.

For the four toxicity prediction tasks with 3D information, following [4], we use multitask learning to jointly tune the four tasks. We also use grid search to find the hyper-parameters, which are left in Appendix B.

Evaluation. For MoleculeNet, we use area under the receiver operating characteristic curve (ROC-AUC). Each experiment is independently run for three times with different seeds, and the mean and standard derivation are reported. Ogb-molpcba has 128 sub-tasks and we use average precision (briefly, AP) as suggested by Hu et al. [14]. For the four toxicity prediction, following [4], we use squared Pearson correlation coefficient (R^2) between the groundtruth and predicted values, rooted mean square error (RMSE) and mean absolute error (MAE) as the evaluation metrics.

Baselines. For MoleculeNet, we compare with three 2D pre-training baselines: AttrMask & ContextPred [15], GROVER [29] and GraphCL [49]. They are all introduced in related work. We also compare with

two 3D pre-training baselines: Stärk et al. [36] and GraphMVP [22], which have been discussed comprehensively. For ogb-molpcba, we mainly compare with Graphormer [48], which is also pre-trained on PCQM4M and achieves the best result on this dataset. For the four toxicity prediction tasks where 3D information is available, we mainly compare with AGBT [4]. Since the Github repository of GraphMVP is empty by the end of the submission, we leave the comparison with it on the four toxicity prediction tasks in the future. We also compare with some classical baselines, which mainly use various molecular fingerprints and multi-task learning.

4.2 Results

The results on MoleculeNet are reported in Table 1. We have the following observations:

(1) Compared with AttrMask & ContextPred [15], GROVER [29] and GraphCL [49] which only leverage the 2D molecular graphs for pre-training, our method outperforms these baselines by large margins. Specifically, on average, our method improves those baselines by 11.81%, 10.50% and 14.08%. This shows the effectiveness of using 3D information in pre-training.

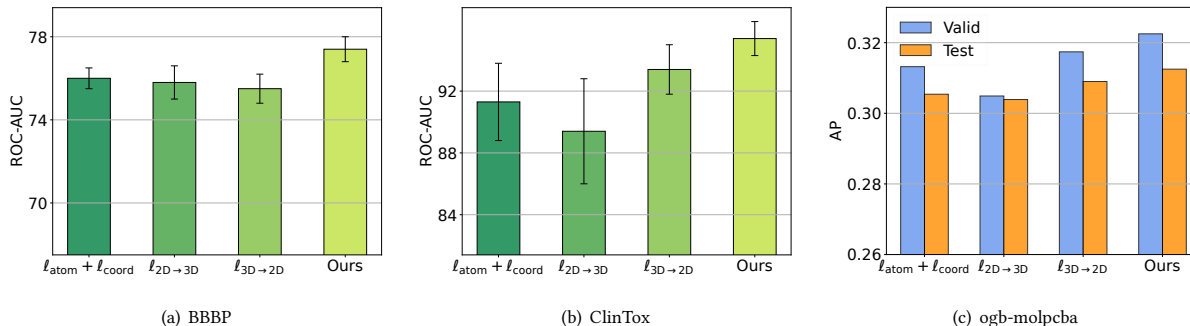
(2) Compared with Stärk et al. [36] and GraphMVP [22], our method still outperforms those baselines. We can improve the average ROC-AUC from 70.37 and 74.65 to 80.85. Stärk et al. [36] and Liu et al. [22] use two separated modules to encode the 2D and 3D information, and they use consistency loss to build their connection. In comparison, we use a unified module to deeply fuse them. The improvement shows that using unified representation is a promising direction for molecule modeling.

The results on ogb-molpcba are summarized in Table 2. We report the results on both validation and test sets following the guidelines [14]. GN [1] and “GIN + virtual node” [21] are two baselines without pre-training, where “GN” is the backbone of our model, and “GIN + virtual node” denotes applying a virtual node, which aggregates the global information of a molecule, into the GIN model [46]. The Graphormer [48] here uses an adversarial augmentation technique named FLAG [21] and obtains good improvements to the non-FLAG version. We also combine FLAG with our method in this work.

We can see that, although ogb-molpcba has more data, it still benefits from pre-training. Compared with GN block, which is the non-pretraining version of network architecture, we can improve the test score from 0.2650 to 0.3125. In addition, by using FLAG, our method outperforms Graphormer by 2.4% and 1.1% on validation and test sets, setting new records for this task.

Table 3: Results of toxicity prediction where both 2D and 3D information is available.

	LD50			LC50			IGC50			LC50DM		
	R^2 (\uparrow)	RMSE (\downarrow)	MAE (\downarrow)	R^2 (\uparrow)	RMSE (\downarrow)	MAE (\downarrow)	R^2 (\uparrow)	RMSE (\downarrow)	MAE (\downarrow)	R^2 (\uparrow)	RMSE (\downarrow)	MAE (\downarrow)
MACCS	0.643	N/A	N/A	0.608	N/A	N/A	0.643	N/A	N/A	0.434	N/A	N/A
Daylight	0.624	N/A	N/A	0.724	N/A	N/A	0.717	N/A	N/A	0.700	N/A	N/A
3D MT-DNN	0.653	0.568	0.421	0.789	0.677	0.446	0.802	0.438	0.305	0.678	0.978	0.714
AGBT	0.671	0.554	0.401	0.783	0.692	0.492	0.842	0.391	0.273	0.830	0.743	0.527
Ours	0.690	0.542	0.399	0.800	0.664	0.444	0.858	0.379	0.263	0.833	0.715	0.475

**Figure 4: Comparison of different pre-training objective functions.**

The results of toxicity prediction with 3D information are reported in Table 3. Compared with AGBT [4], our method outperforms this strong baseline on all the four tasks and evaluation metrics. Chen et al. [4] separately deal with the 2D graph and 3D conformation, while we use a unified model to extract representations of the input molecule that can more consistently utilize the two types of information. Our method also outperforms the non-pretraining methods, including the 2D fingerprint baselines like MACCS [8], Daylight (reported by [10]), and the 3D based methods like 3D MT-DNN [44]. This shows that the molecular representation obtained by pre-training outperforms the manually designed fingerprints. These results demonstrate the effectiveness of our proposed method for molecular property prediction.

4.3 Ablation Study

We mainly focus on the following questions:

(Q1) What is the contribution of each training objective function?

(Q2) What is the effect of different mask ratios?

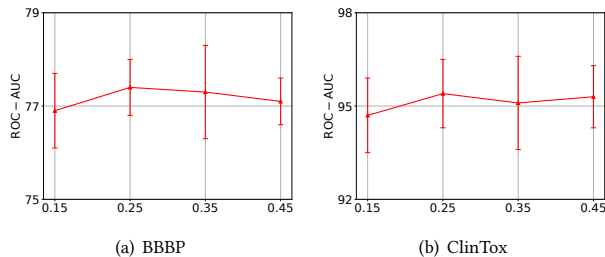
To answer (Q1), we independently pre-train the models with $l_{\text{atom}} + l_{\text{coord}}$, $l_{2D \rightarrow 3D}$ and $l_{3D \rightarrow 2D}$, respectively. After that, we fine-tune the obtained models on the MoleculeNet datasets and ogb-molpcba. Part of the results are summarized in Figure 4 and the remaining ones are left in Appendix C. We can see that:

(1) If we independently use any one of $l_{\text{atom}} + l_{\text{coord}}$, $l_{2D \rightarrow 3D}$ and $l_{3D \rightarrow 2D}$, the performance is not as good as using them together. This shows that each of them contribute to the unified pre-training and we should combine them together.

(2) Reconstructing the masked atoms and coordinates is relatively more important for the unified pre-training. However, it is ignored

by previous works [22, 36], which mainly focus on preserving the consistency of different views.

(3) According to our statistics, the average ROC-AUC scores on MoleculeNet of the above three loss functions are 79.15, 78.57 and 79.21. All of them are better than [22, 36], which demonstrate the power of unified representations.

**Figure 5: Results of different masked ratios p .**

To answer (Q2), we try 4 different mask ratios, 0.15, 0.25, 0.35 and 0.45. We conduct experiments on the BBBP and ClinTox from MoleculeNet. The results are shown in Figure 5. In general, our pre-training method is robust to the choice of the mask ratios. For example, on BBBP, the maximum performance gap among the four ratios is 0.5. Empirically, setting p as 0.25 achieves the best results.

When only 2D information is available, people might be curious about the initialization of the 3D coordinates. By default, we uniformly sample the coordinates from $[-1, 1]$. To verify its robustness, on ogb-molpcba, we randomly sample ten groups of initial coordinates and evaluate them. We also set all the initial coordinates

Table 4: Experimental results on conformation generation.

Dataset Methods	QM9				Drugs			
	COV(%) \uparrow		MAT (Å) \downarrow		COV(%) \uparrow		MAT (Å) \downarrow	
	Mean	Median	Mean	Median	Mean	Median	Mean	Median
RDKit	83.26	90.78	0.3447	0.2935	60.91	65.70	1.2026	1.1252
GraphDG [35]	73.33	84.21	0.4245	0.3973	8.27	0.00	1.9722	1.9845
ConfGF [33]	88.49	94.13	0.2673	0.2685	62.15	70.93	1.1629	1.1596
DGSM [25]	91.49	95.92	0.2139	0.2137	78.73	94.39	1.0154	0.9980
GeoDiff [47]	91.68	95.82	0.2099	0.2021	89.13	97.88	0.8629	0.8529
DMCG [52]	96.34	99.53	0.2065	0.2003	96.69	100.00	0.7223	0.7236
Ours	96.93	100.00	0.1958	0.1849	97.05	100.00	0.7056	0.6973

zero and check the inference result. The differences of the above 11 trials are less than 10^{-4} , which shows that our model is robust to the initial coordinates.

5 APPLICATION TO CONFORMATION GENERATION

In this section, we conduct experiments on 3D conformation generation, which is to map the 2D molecular graph to 3D conformation.

5.1 Settings

Following [25, 35, 47], we use a subset of GEOM-QM9 and GEOM-Drugs [3] to evaluate our method. The numbers of training, validation and test (molecule, conformation) pairs of GEOM-QM9 are 200K, 2.5K and 22408 respectively, while those numbers for GEOM-Drugs are 200K, 2.5K and 14324. On average, GEOM-QM9 and GEOM-Drugs have 8.8 and 24.9 heavy atoms respectively.

Considering each molecular corresponds to multiple diverse conformations, we adopt the variational auto-encoder framework and generate multiple conformations. We choose the model proposed by Zhu et al. [51] for conformation generation, and the parameters are initialized by our pre-trained unified model. The model is a 12-layer network with hidden dimension 256. We also use Adam optimizer for training with learning rate 10^{-4} and the model is finetuned for 100 epochs.

We evaluate the diversity and accuracy of generated conformations. Let $\text{RMSD}(R, \hat{R})$ denote the root mean square deviations of two conformations R and \hat{R} :

$$\text{RMSD}(R, \hat{R}) = \min_{\Phi} \left(\frac{1}{|V|} \sum_{i=1}^{|V|} \|R_i - \Phi(\hat{R}_i)\|^2 \right)^{\frac{1}{2}}, \quad (8)$$

where Φ is the alignment function that aligns two conformations by roto-translation operations. We use the coverage score (COV) and matching score (MAT) for evaluation. Let S_g and S_r denote the collections of the generated conformations and the groundtruth conformations. Assume in the test set, the molecule m has N_m conformations, following [25, 33], we generate $2N_m$ conformations for it. Mathematically, $\text{COV}(S_g, S_r)$ and $\text{MAT}(S_g, S_r)$ are defined as follows:

$$\begin{aligned} \text{COV}(S_g, S_r) &= \frac{1}{|S_r|} |\{R \in S_r \mid \text{RMSD}(R, \hat{R}) < \delta, \exists \hat{R} \in S_g\}|; \\ \text{MAT}(S_g, S_r) &= \frac{1}{|S_r|} \sum_{R \in S_r} \min_{\hat{R} \in S_g} \text{RMSD}(R, \hat{R}). \end{aligned} \quad (9)$$

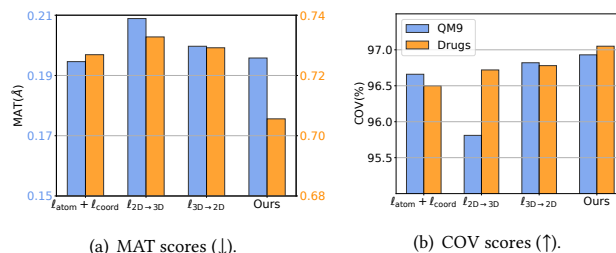


Figure 6: Comparison of different pre-training objective functions on conformation generation tasks.

Following previous works [33, 47], δ 's are set as 0.5 and 1.25 for GEOM-QM9 and GEOM-Drugs datasets, respectively.

5.2 Results

The results are reported in Table 4. We can see that our method outperforms all previous baselines, no matter for distance-based methods like ConfGF [33], DGSM [25], or the recently proposed direct approach [51]. This shows the effectiveness of our pre-training in conformation generation.

Similar to the first question in Section 4.3, we also conduct ablation study of different training objective functions. The results are shown in Figure 6. For the MAT scores, the values of QM9 correspond to the left axis, and those of Drugs correspond to the right axis. We get the same conclusion as Section 4.3: Using all the three types of loss function together achieves the best performance.

6 CONCLUSIONS AND FUTURE WORK

In this work, we propose the unified 2D and 3D pre-training, that jointly leverages the 2D graph structure of the molecule and the 3D conformation. We design three loss functions, including reconstructing the masked atoms and coordinates, 2D graph to 3D conformation generation and the 3D conformation to 2D graph generation. The permutation invariance and roto-translation invariance are considered. We conduct experiments on 11 molecular property prediction tasks and 2 conformation generation tasks, and achieve state-of-the-art results on 12 of them.

For future work, first, we will explore how to leverage the large amount of molecules without 3D structures. We could use them to enhance the ℓ_{atom} and use cycle consistency loss, where we map

the 2D graph G to 3D conformation \hat{R} and then map \hat{R} back to 2D graph \hat{G} . G and \hat{G} should preserve enough similarity. Second, the combination of our method with contrastive learning is another topic. Third, we will apply our pre-trained model to more scenarios like drug-drug interaction and drug-target interaction prediction.

ACKNOWLEDGMENTS

This work was supported in part by the National Natural Science Foundation of China under Contract 61836011 and in part by the Youth Innovation Promotion Association CAS under Grant 2018497.

REFERENCES

- [1] Ravichandra Addanki, Peter W Battaglia, David Budden, Andreea Deac, Jonathan Godwin, Thomas Keck, Wai Lok Sibon Li, Alvaro Sanchez-Gonzalez, Jacklynn Stott, Shantanu Thakoor, et al. 2021. Large-scale graph representation learning with very deep GNNs and self-supervision. *arXiv:2107.09422* (2021).
- [2] Brandon Anderson, Truong Son Hy, and Risi Kondor. 2019. Cormorant: Covariant molecular neural networks. *NeurIPS* 32 (2019).
- [3] Simon Axelrod and Rafael Gomez-Bombarelli. 2020. Geom: Energy-annotated molecular conformations for property prediction and molecular generation. *arXiv preprint arXiv:2006.05531* (2020).
- [4] Dong Chen, Kaifu Gao, Duc Duy Nguyen, Xin Chen, Yi Jiang, Guo-Wei Wei, and Feng Pan. 2021. Algebraic graph-assisted bidirectional transformers for molecular property prediction. *Nature Communications* 12, 1 (2021), 1–9.
- [5] Seyone Chithrananda, Gabriel Grand, and Bharath Ramsundar. 2020. Chemberta: Large-scale self-supervised pretraining for molecular property prediction. *arXiv:2010.09885* (2020).
- [6] Jacob Devlin, Ming-Wei Chang, Kenton Lee, and Kristina Toutanova. 2019. BERT: Pre-training of Deep Bidirectional Transformers for Language Understanding. In *NAACL*. 4171–4186.
- [7] Alexey Dosovitskiy, Lucas Beyer, Alexander Kolesnikov, Dirk Weissenborn, Xi-aohua Zhai, Thomas Unterthiner, Mostafa Dehghani, Matthias Minderer, Georg Heigold, Sylvain Gelly, Jakob Uszkoreit, and Neil Houlsby. 2021. An Image is Worth 16x16 Words: Transformers for Image Recognition at Scale. In *ICLR*.
- [8] Joseph L. Durant, Burton A. Leland, Douglas R. Henry, and James G. Nourse. 2002. Reoptimization of MDL Keys for Use in Drug Discovery. *Journal of Chemical Information and Computer Sciences* 42, 6 (2002), 1273–1280.
- [9] Fabian Fuchs, Daniel Worrall, Volker Fischer, and Max Welling. [n. d.]. SE(3)-Transformers: 3D Roto-Translation Equivariant Attention Networks. In *NeurIPS*.
- [10] Kaifu Gao, Duc Duy Nguyen, Vishnu Sresht, Alan M. Mathiowetz, Meihua Tu, and Guo-Wei Wei. 2020. Are 2D fingerprints still valuable for drug discovery? *Phys. Chem. Chem. Phys.* 22 (2020), 8373–8390. Issue 16.
- [11] Justin Gilmer, Samuel S. Schoenholz, Patrick F. Riley, Oriol Vinyals, and George E. Dahl. 2017. Neural Message Passing for Quantum Chemistry. In *ICML*. 1263–1272.
- [12] Shion Honda, Shoi Shi, and Hiroki R Ueda. 2019. Smiles transformer: Pre-trained molecular fingerprint for low data drug discovery. *arXiv:1911.04738* (2019).
- [13] Weihua Hu, Matthias Fey, Hongyu Ren, Maho Nakata, Yuxiao Dong, and Jure Leskovec. 2021. OGB-LSC: A Large-Scale Challenge for Machine Learning on Graphs. In *Thirty-fifth Conference on Neural Information Processing Systems Datasets and Benchmarks Track (Round 2)*.
- [14] Weihua Hu, Matthias Fey, Marinka Zitnik, Yuxiao Dong, Hongyu Ren, Bowen Liu, Michele Catasta, and Jure Leskovec. 2020. Open Graph Benchmark: Datasets for Machine Learning on Graphs. *arxiv abs/2005.00687* (2020).
- [15] Weihua Hu, Bowen Liu, Joseph Gomes, Marinka Zitnik, Percy Liang, Vijay Pande, and Jure Leskovec. 2020. Strategies for Pre-training Graph Neural Networks. In *ICLR*.
- [16] Sergey Ioffe and Christian Szegedy. 2015. Batch Normalization: Accelerating Deep Network Training by Reducing Internal Covariate Shift. In *ICML*, Vol. 37. Lille, France, 448–456.
- [17] Wengong Jin, Jonathan M. Stokes, Richard T. Eastman, Zina Itkin, Alexey V. Zakharov, James J. Collins, Tommi S. Jaakkola, and Regina Barzilay. 2021. Deep learning identifies synergistic drug combinations for treating COVID-19. *Proceedings of the National Academy of Sciences* 118, 39 (2021).
- [18] Lukasz Kaiser, Aidan N. Gomez, Noam Shazeer, Ashish Vaswani, Niki Parmar, Llion Jones, and Jakob Uszkoreit. 2017. One Model To Learn Them All. *CoRR abs/1706.05137* (2017). [arXiv:1706.05137](https://arxiv.org/abs/1706.05137)
- [19] Charles FF Karney. 2007. Quaternions in molecular modeling. *Journal of Molecular Graphics and Modelling* 25, 5 (2007), 595–604.
- [20] Johannes Klicpera, Janek Groß, and Stephan Günnemann. 2020. Directional Message Passing for Molecular Graphs. In *ICLR*.
- [21] Kezhi Kong, Guohao Li, Mucong Ding, Zuxuan Wu, Chen Zhu, Bernard Ghanem, Gavin Taylor, and Tom Goldstein. 2020. FLAG: Adversarial Data Augmentation for Graph Neural Networks. *CoRR abs/2010.09891* (2020).
- [22] Shengchao Liu, Hanchen Wang, Weiyang Liu, Joan Lasenby, Hongyu Guo, and Jian Tang. 2022. Pre-training Molecular Graph Representation with 3D Geometry. In *ICLR*.
- [23] Yinhan Liu, Myle Ott, Naman Goyal, Jingfei Du, Mandar Joshi, Danqi Chen, Omer Levy, Mike Lewis, Luke Zettlemoyer, and Veselin Stoyanov. 2019. Roberta: A robustly optimized bert pretraining approach. *arXiv:1907.11692* (2019).
- [24] Chengqiang Lu, Qi Liu, Chao Wang, Zhenya Huang, Peize Lin, and Lixin He. 2019. Molecular property prediction: A multilevel quantum interactions modeling perspective. In *AAAI*, Vol. 33. 1052–1060.
- [25] Shitong Luo, Chence Shi, Minkai Xu, and Jian Tang. 2021. Predicting Molecular Conformation via Dynamic Graph Score Matching. In *NeurIPS*, Vol. 34.
- [26] Elman Mansimov, Omar Mahmood, Seokho Kang, and Kyunghyun Cho. 2019. Molecular Geometry Prediction using a Deep Generative Graph Neural Network. *Scientific Reports* 9, 1 (31 Dec 2019), 20381.
- [27] Rocco Meli and Philip C. Biggin. 2020. spyrmsd: symmetry-corrected RMSD calculations in Python. *Journal of Cheminformatics* 12, 1 (31 Aug 2020), 49.
- [28] Aditya Ramesh, Mikhail Pavlov, Gabriel Goh, Scott Gray, Chelsea Voss, Alec Radford, Mark Chen, and Ilya Sutskever. 2021. Zero-Shot Text-to-Image Generation. In *ICML*, Vol. 139. 8821–8831.
- [29] Yu Rong, Yatao Bian, Tingyang Xu, Weiyang Xie, Ying WEI, Wenbing Huang, and Junzhou Huang. 2020. Self-Supervised Graph Transformer on Large-Scale Molecular Data. In *NeurIPS*, Vol. 33. 12559–12571.
- [30] Kristof Schütt, Oliver Unke, and Michael Gastegger. 2021. Equivariant message passing for the prediction of tensorial properties and molecular spectra. In *ICML*.
- [31] K. T. Schütt, P.-J. Kindermans, H. E. Sauceda, S. Chmiela, A. Tkatchenko, and K.-R. Müller. 2017. SchNet: A Continuous-Filter Convolutional Neural Network for Modeling Quantum Interactions. In *NeurIPS* (Long Beach, California, USA). Curran Associates Inc., Red Hook, NY, USA, 992–1002.
- [32] Hari Om Sharan. 2021. *Artificial Intelligence in Bioinformatics*. Springer Singapore, Singapore, 395–403. https://doi.org/10.1007/978-981-33-6191-1_21
- [33] Chence Shi, Shitong Luo, Minkai Xu, and Jian Tang. 2021. Learning gradient fields for molecular conformation generation. In *ICML*. PMLR, 9558–9568.
- [34] Zeren Shui and George Karypis. 2020. Heterogeneous molecular graph neural networks for predicting molecule properties. In *ICDM*. IEEE, 492–500.
- [35] Gregor Simm and Jose Miguel Hernandez-Lobato. 2020. A Generative Model for Molecular Distance Geometry. In *ICML*, Vol. 119. PMLR, 8949–8958.
- [36] Hannes Stärk, Dominique Beaini, Gabriele Corso, Prudencio Tossou, Christian Dallago, Stephan Günnemann, and Pietro Liò. 2021. 3D Infomax improves GNNs for Molecular Property Prediction. *arXiv preprint arXiv:2110.04126* (2021).
- [37] Hannes Stärk, Dominique Beaini, Gabriele Corso, Prudencio Tossou, Christian Dallago, Stephan Günnemann, and Pietro Liò. 2021. 3D Infomax improves GNNs for Molecular Property Prediction. *CoRR abs/2110.04126* (2021).
- [38] Jonathan M Stokes, Kevin Yang, Kyle Swanson, Wengong Jin, Andres Cubillos-Ruiz, Nina M Donghia, Craig R MacNair, Shawn French, Lindsey A Carfrae, Zohar Bloom-Ackermann, et al. 2020. A deep learning approach to antibiotic discovery. *Cell* 180, 4 (2020), 688–702.
- [39] Igor V. Tetko and Ola Engkvist. 2020. From Big Data to Artificial Intelligence: cheminformatics meets new challenges. *Journal of Cheminformatics* 12, 1 (18 Dec 2020), 74. <https://doi.org/10.1186/s13321-020-00475-y>
- [40] Ashish Vaswani, Noam Shazeer, Niki Parmar, Jakob Uszkoreit, Llion Jones, Aidan N Gomez, Łukasz Kaiser, and Illia Polosukhin. 2017. Attention is All you Need. In *NeurIPS*.
- [41] Sheng Wang, Yuzhi Guo, Yuhong Wang, Hongmao Sun, and Junzhou Huang. 2019. Smiles-bert: large scale unsupervised pre-training for molecular property prediction. In *Proceedings of the 10th ACM international conference on bioinformatics, computational biology and health informatics*. 429–436.
- [42] Yuyang Wang, Jianren Wang, Zhonglin Cao, and Amir Barati Farimani. 2021. MolCLR: molecular contrastive learning of representations via graph neural networks. *arXiv preprint arXiv:2102.10056* (2021).
- [43] David Weininger. 1988. SMILES, a chemical language and information system. 1. Introduction to methodology and encoding rules. *Journal of Chemical Information and Computer Sciences* 28, 1 (1988), 31–36. <https://doi.org/10.1021/ci00057a005>
- [44] Kedi Wu and Guo-Wei Wei. 2018. Quantitative Toxicity Prediction Using Topology Based Multitask Deep Neural Networks. *Journal of Chemical Information and Modeling* 58, 2 (2018), 520–531.
- [45] Zhenqin Wu, Bharath Ramsundar, Evan N Feinberg, Joseph Gomes, Caleb Geniesse, Aneesh S Pappu, Karl Leswing, and Vijay Pande. 2018. MoleculeNet: a benchmark for molecular machine learning. *Chemical science* 9, 2 (2018), 513–530.
- [46] Keyulu Xu, Weihua Hu, Jure Leskovec, and Stefanie Jegelka. 2019. How Powerful are Graph Neural Networks?. In *ICLR* 2019.
- [47] Minkai Xu, Lantao Yu, Yang Song, Chence Shi, Stefano Ermon, and Jian Tang. 2022. GeoDiff: A Geometric Diffusion Model for Molecular Conformation Generation. In *ICLR*.
- [48] Chengxuan Ying, Tianle Cai, Shengjie Luo, Shuxin Zheng, Guolin Ke, Di He, Yanming Shen, and Tie-Yan Liu. 2021. Do Transformers Really Perform Badly for Graph Representation?. In *Advances in Neural Information Processing Systems*.
- [49] Yuning You, Tianlong Chen, Yongduo Sui, Ting Chen, Zhangyang Wang, and Yang Shen. 2020. Graph Contrastive Learning with Augmentations. In *NeurIPS*.

- [50] Hengshuang Zhao, Li Jiang, Jiaya Jia, Philip HS Torr, and Vladlen Koltun. 2021. Point transformer. In *ICCV*. 16259–16268.
- [51] Jinhua Zhu, Yingce Xia, Chang Liu, Lijun Wu, Shufang Xie, Tong Wang, Yusong Wang, Wengang Zhou, Tao Qin, Houqiang Li, and Tie-Yan Liu. 2022. Direct molecular conformation generation. *arXiv preprint arXiv:2202.01356* (2022).
- [52] Jinhua Zhu, Yingce Xia, Tao Qin, Wengang Zhou, Houqiang Li, and Tie-Yan Liu. 2021. Dual-view molecule pre-training. *arXiv preprint arXiv:2106.10234* (2021).

A DETAILS ABOUT THE NETWORK

As introduced in Section 3.3, the model is a stack of L identical blocks, where each block takes the output of the previous one as input. The $(l-1)$ -th block will output the representations of atom v_i (denoted as $x_i^{(l-1)} \in \mathbb{R}^d$), the representations of bond e_{ij} (denoted as $x_{ij}^{(l-1)} \in \mathbb{R}^d$), a predicted conformation $\hat{R}^{(l-1)}$, and a global representation of the molecule $u^{(l-1)}$. Let $\mathcal{N}(i)$ denote the neighbors of atom i , i.e., $\mathcal{N}(i) = \{j \mid e_{ij} \in E\}$. The workflow of the l -th block is shown as follows:

(1) *Incorporate geometric information:*

$$\begin{aligned}\bar{x}_i^{(l)} &= x_i^{(l-1)} + \text{FF}(\hat{R}_i^{(l-1)}), \\ \bar{x}_{ij}^{(l)} &= x_{ij}^{(l-1)} + \text{FF}(\|\hat{R}_i^{(l-1)} - \hat{R}_j^{(l-1)}\|).\end{aligned}\quad (10)$$

(2) *Update bond representations:* For each $e_{ij} \in E$,

$$x_{ij}^{(l)} = x_{ij}^{(l-1)} + \text{FF}(\bar{x}_i^{(l-1)}, \bar{x}_j^{(l-1)}, \bar{x}_{ij}^{(l)}, u^{(l-1)}). \quad (11)$$

(3) *Update atom representations:* For any $i \in V$,

$$\begin{aligned}\tilde{x}_i^{(l)} &= \sum_{j \in \mathcal{N}(i)} \alpha_j W_v [x_{ij}^{(l)}; \bar{x}_j^{(l)}]; \\ \alpha_j &\propto \exp(\mathbf{a}^\top \xi (W_q \bar{x}_i^{(l-1)} + W_k [\bar{x}_j^{(l-1)}; \bar{x}_{ij}^{(l)}])); \\ x_i^{(l)} &= x_i^{(l-1)} + \text{MLP}(x_i^{(l-1)}, \tilde{x}_i^{(l)}, u^{(l-1)}).\end{aligned}\quad (12)$$

In Eqn.(12), \mathbf{a} , W_q , W_v and W_k are the parameters to be learned, $[a; b]$ is the concatenation of two vectors a and b , and ξ is the leaky ReLU activation.

(4) *Update global representations:* The global representations are updated by aggregating the new bond representations and atom representations, i.e.,

$$u^{(l)} = u^{(l-1)} + \text{FF}\left(\frac{1}{|V|} \sum_{i=1}^{|V|} x_i^{(l)}, \frac{1}{|E|} \sum_{i,j} x_{ij}^{(l)}, u^{(l-1)}\right). \quad (13)$$

After obtaining the updated representations, the l -th block predicts a new 3D conformation. For any $i \in \{1, 2, \dots, |V|\}$,

$$\begin{aligned}\Delta_i^{(l)} &= \text{FF}(x_i^{(l)}), \quad \mu^{(l)} = \frac{1}{|V|} \sum_{j=1}^{|V|} \Delta_j^{(l)}, \\ \hat{R}_i^{(l)} &= \hat{R}_i^{(l-1)} + (\Delta_i^{(l)} - \mu^{(l)}).\end{aligned}\quad (14)$$

B FINETUNING HYPERPARAMETERS

We summarize the finetuning hyperparameters in Table 5. The hyperparameters for the six tasks from MoleculeNet are in the ‘‘MoleculeNet’’ column, while those for the four toxicity prediction tasks are in the ‘‘Toxicity’’ column.

The details of the dataset are in Table 7.

Hyper parameters	MoleculeNet	Toxicity
Learning Rate	{2e-4, 5e-4, 8e-4, 1e-3}	{5e-4, 8e-4, 1e-3, 2e-3}
Dropout	{0.3, 0.4, 0.5}	{0.2, 0.3, 0.4, 0.5}
Batch Size	{16, 32, 64, 128}	{16, 32, 64}
Max Epochs	{10, 20, 50}	{10, 20, 50, 100}
Weight Decay	{0.01, 0.1}	{0.01, 0.1}

Table 5: Finetuning hyperparameters.

C PRE-TRAINING WITH DIFFERENT LOSS FUNCTION

Dataset	BBBP	Tox21	ClinTox
$\ell_{\text{atom}} + \ell_{\text{coord}}$	76.0 \pm 0.5	75.5 \pm 0.4	91.3 \pm 2.5
$\ell_{2\text{D} \rightarrow 3\text{D}}$	75.8 \pm 0.8	74.7 \pm 0.6	89.4 \pm 3.4
$\ell_{3\text{D} \rightarrow 2\text{D}}$	75.5 \pm 0.7	75.0 \pm 0.4	93.4 \pm 1.6
Ours	77.3 \pm 0.4	75.9 \pm 0.3	95.0 \pm 1.1
Dataset	HIV	BACE	SIDER
$\ell_{\text{atom}} + \ell_{\text{coord}}$	81.2 \pm 1.4	85.1 \pm 0.5	65.8 \pm 1.3
$\ell_{2\text{D} \rightarrow 3\text{D}}$	81.0 \pm 1.3	85.3 \pm 1.3	65.2 \pm 0.8
$\ell_{3\text{D} \rightarrow 2\text{D}}$	80.9 \pm 1.2	85.4 \pm 1.5	65.1 \pm 1.5
Ours	82.2 \pm 1.0	86.8 \pm 0.6	67.4 \pm 0.5

Table 6: Ablation study of different training objective functions on MoleculeNet.

As introduced in Section 4.3, we conduct ablation study of pre-training with different objective functions, and finetuning on MoleculeNet. The results are summarized in Table 6. We can see that independently using any objective is not as good as combining them together.

Table 7: Details about the datasets for molecular property prediction.

Dataset	3D	#Instance	Description	Evaluation
BBBP	N	2053	Prediction of the barrier permeability of the small molecules.	ROC-AUC
Tox21	N	8014	Qualitative toxicity measurements on 12 different targets.	ROC-AUC
ClinTox	N	1491	The prediction of clinical trial toxicity and FDA approval status.	ROC-AUC
HIV	N	41913	Prediction of the ability to inhibit HIV replication.	ROC-AUC
BACE	N	1522	Prediction of binding results for a set of inhibitors of human β -secretase 1.	ROC-AUC
SIDER	N	1427	The side effect of drugs.	ROC-AUC
PCBA	N	437929	Prediction of biological activities obtained by HTS.	Average Precision (AP)
LD50	Y	7413	The amount of chemicals that can kill half of the rats when orally ingested.	R^2 /RMSE/MAE
LGC50	Y	1792	50% growth inhibitory concentration of Tetrahymena pyriformis organism after 40h.	R^2 /RMSE/MAE
LC50	Y	823	The concentration of test chemicals in water that causes 50% of fathead minnows to die after 96h.	R^2 /RMSE/MAE
LC50DM	Y	353	The concentration of test chemicals in water that causes 50% Daphnia Magna to die after 48h.	R^2 /RMSE/MAE